Electronic Supplementary Material (ESI) for Journal of Materials Chemistry A.

Supporting Information

Ultrathin NiCo2Px nanosheets strongly coupled with CNTs as efficient and robust electrocatalysts for overall water splitting

Can Huang[a], *Ting Ouyang*[a], *Ying Zou*[a], *Nan Li*[a], *Zhao-Qing Liu*[a*]

[a]School of Chemistry and Chemical Engineering/Guangzhou Key Laboratory for Environmentally Functional Materials and Technology/Key Laboratory for Water Quality and Conservation of the Pearl River Delta, Ministry of Education, Guangzhou University, Guangzhou Higher Education Mega Center, Outer Ring Road No. 230, 510006, P. R. China.

Contents

1. Experimental Section

2. Supplementary Figures

3. Supplementary Tables

1. Experimental Section

1.1 Materials

All reagents used in the experiment are of analytical grade and used without further purification. $Ni(NO_3)_2 \cdot 6H_2O$ (99% AR) and $Co(NO_3)_2 \cdot 6H2O$ (99% AR) were obtained from Sinopharm Chemical Reagent Co., Ltd. IrO_2 (85 wt.%) and Pt/C (20 wt.%) were obtained from Shanghai Hansi Chemical Industry Co., Ltd. Polyvinylpyrrolidone (PVP, 99% AR) was obtained from Shanghai Tianlian Fine Chemical Co. Ltd. $NH_3 \cdot H_2O$ (25–28 wt%) and $NaH_2PO_2 \cdot H_2O$ (99% AR) were obtained from Tianjin Fuyu Fine Chemical Co. Ltd. Multi-walled carbon nanotubes (CNTs, 99% AR) were purchased from Shenzhen Nanotech Port Co. Ltd.

1.2 Synthesis of catalysts

1.2.1 *Preparation of functionalized carbon nanotubes*

Functionalized carbon nanotubes (CNT) was prepared by a modified Hummers method[1]. Briefly, 23 mL concentrated sulfuric acid was added to CNTs and stirred for overnight. Then, 416 mg of KNO_3 was added, followed by the slow addition of 1 g of $KMnO_4$ at 40 ℃. The mixture was kept stirring at 40 ℃ for 30 min. Subsequently, 3 mL of double-distilled water was added to the flask, followed by another 3 mL of double-distilled water after 3 minutes. After another 3 minutes, 40 mL of double-distilled water was added. After continuously stirring for 30 minutes, 140 mL of double-distilled water and 10 mL of H_2O_2 (30 %) were added to terminate the oxidization reaction. The oxidized CNTs were collected, repetitively washed with 5 % HCl solution and double-distilled water, and finally lyophilized.

1.2.2 *Synthesis of 3D bouquet-like $NiCo_2O_4$/CNTs*

In a typical synthesis, 0.87 g of $Ni(NO_3)_2·6H_2O$ and 1.74 g of $Co(NO_3)_2·6H_2O$ were dissolved in 50 mL H_2O to form a clear purple solution, which was then mixed with 0.1 g PVP. After that, 0.05 g of functionalized CNTs powder was uniformly dispersed in the aqueous solution with the assistance of ultrasonication at 400 W for 30 min. Then, $NH_3·H_2O$ (5%) was added dropwise until pH reached 9. The obtained precipitate was filtered, washed with water and ethanol several times to remove the surfactant and residual ions, and dried at 40 ℃ for 12 h under vacuum. Finally, the hybrid precursor was annealed in air at 250 ℃ for 2 h with a heating rate of 2 ℃ min^{-1}. The yield of the catalyst was 92%. The obtained catalyst is denoted as $NiCo_2O_4$/CNTs, NiO/CNTs and Co_3O_4/CNTs were synthesized by a similar method except for 2.61 g of $Ni(NO_3)_2·6H_2O$ and $Co(NO_3)_2·6H_2O$ served as nickel and cobalt source, respectively. Bulk $NiCo_2O_4$ was prepared by a similar synthesis procedure without the addition of the functionalized CNTs.

1.2.3 *Synthesis of 3D bouquet-like $NiCo_2P_x$/CNTs*

To prepare $NiCo_2P_x$/CNTs, $NiCo_2O_4$/CNTs and NaH_2PO_2 were put at two separate positions in a porcelain boat with NaH_2PO_2 at the upstream side of the furnace. The mass ratio for $NiCo_2O_4$/CNTs to NaH_2PO_2 was 1:5. After flushed with Ar for 2 h, the center of the furnace was elevated to 300 °C at a ramping rate of 1 °C min^{-1} and held at this temperature for 2 h, and then naturally cooled to ambient temperature under Ar.

1.2.4 *Synthesis of NiP_x/CNTs, CoP_x/CNTs, and bulk $NiCo_2P_x$.*

The synthesis of NiP_x/CNTs, CoP_x/CNTs and bulk $NiCo_2P_x$ were similar as that of $NiCo_2P_x$/CNTs except for NiO/CNTs, Co_3O_4/CNTs, and bulk $NiCo_2O_4$ were respectively used to instead of $NiCo_2O_4$/CNTs.

1.2.5 *Synthesis of bulk $NiCo_2P_x$+CNTs*

The physically mixed bulk $NiCo_2P_x$+CNTs was similar as that of $NiCo_2P_x$/CNTs except the step of adding functionalized CNTs is postponed until filter.

1.3 Characterizations

The morphology of the as-prepared $NiCo_2P_x$/CNTs composites was analyzed by field emission scanning electron microscopy (FE-SEM, JEOL JSM-7001F) and transmission electron microscopy (TEM, JEM2010-HR). The crystal structure of the as-prepared samples was analyzed by X-ray diffraction (XRD, PANalytical, PW3040/60) with Cu Kα radiation (λ = 0.15418 nm). Detailed chemical composition of samples was analyzed by X-ray photoelectron spectroscopy (XPS, ESCALab250). The Raman spectra were collected on a Raman spectrometer (JY, HR 800) using 514-nm laser. Nitrogen adsorption-desorption isotherm was collected on Tristar II (Micrometrics) at 77 K. The specific surface area and pore size distribution of the samples were investigated using the Brunauer-Emmett-Teller (BET) method. Pore size distribution of the materials was obtained by Barrett-Joyner-Halenda (BJH) model using the adsorption branch of the isotherm.

1.4 Electrochemical measurements

1.4.1 Electrode preparation

The HER and OER electrochemical analysis were performed under identical conditions with the same catalyst mass loading. 6 mg of the as-synthesized catalyst was first ultrasonically dispersed in a mixture of 1.5 mL DI water and 1.44 mL ethanol followed by the addition of 60 µL of Nafion® solution (5.0 wt%). Then, 9.8 µL of the catalyst dispersion (2 mg mL^{-1}) was transferred onto the glassy carbon rotating disk electrode (RDE, 0.196 cm^2), following by solvent evaporation in air for 2 h. The resulting electrode was served as the working electrode.

1.4.2 Electrochemical testing

The electrochemical properties of the as-prepared samples were investigated using an AMETEK Princeton Applied Research ParSTAT MC 2000A equipped with a rotation disk electrode (glassy carbon, 0.196 cm^{-2}). A graphite rod serves as a counter electrode, Hg/HgO electrode as the reference electrode and the samples as working electrodes. The electrolyte was 1 M KOH (pH = 14) and 1 M PBS (pH=7). All potentials were converted to reversible hydrogen electrode (RHE) following the Nernst equation:

$$E_{RHE}(V) = E_{Hg/HgO} + 0.098 + 0.059 \times pH$$

HER and OER polarization curves were recorded at the scan rate of 5 mV s^{-1}. The working electrodes were cycled at 5 mV s^{-1} until a stable cyclic voltammetry (CV) was achieved before we collected the data. All polarization curves were corrected for the *IR* compensation. Electrochemical impedance spectroscopy (EIS) was performed at open circuit potential (OCP) in the frequency range of 1 Hz to 100000 Hz.

1.4.3 *Electrochemical active surface area (ECSA)*

Electrochemical capacitance was measured using CV measurements. The currents were measured in a narrow potential window that no faradaic processes were observed. CVs were collected at different scan rates: 5, 10, 20, 30, 40, and 50 mV s^{-1}. The measured current in this non-Faradaic potential region should be mostly due to the charging of the double-layer. By plotting the capacitive currents ($\Delta j = j_a - j_c$) against the scan rate and following with a linear fit, the double layer capacitance C_{dl} is around half of the slope. The ECSA can be further estimated from C_{dl} normalized by a specific capacitance for a flat surface, which is normally between 0.02-0.06 mF cm^{-2}. Here we used 40 μF cm^{-2} as the standard for the ECSA estimation and the turnover frequency calculation in section 1.4.4.

1.4.4 *Turnover frequency (TOF) calculations*

TOF was calculated by a previous method[2], according to the following formula:

$$\text{TOF} = \frac{\text{Number of total hydrogen (or oxygen) turn overs / geometric area (cm2)}}{\text{Number of active sites / geometric area (cm2)}}$$

(1)

The number of the total hydrogen (or oxygen) turn overs can be calculated based on the current density (*j*, *IR*-corrected) according to:

$$\text{Number of H2} = j \times \frac{1C\,s^{-1}}{1000\,mA} \times \frac{1\,mol\,e}{96485.3\,C} \times \frac{1\,mol\,\text{H2}}{2\,mol\,e} \times \frac{6.022 \times 1023\ \text{H2 molecules}}{1\,mol\,\text{H2}}$$

$$= j \times 3.12 \times 1015\ \text{H2 molecules}\ mA^{-1}s^{-1} \qquad \textbf{(2)}$$

$$\text{Number of O2} = j \times \frac{1C\,s^{-1}}{1000\,mA} \times \frac{1\,mol\,e}{96485.3\,C} \times \frac{1\,mol\,\text{O2}}{4\,mol\,e} \times \frac{6.022 \times 1023\ \text{O2 molecules}}{1\,mol\,\text{O2}}$$

$$= j \times 1.56 \times 1015\ \text{O2 molecules}\ mA^{-1}s^{-1} \qquad \textbf{(3)}$$

Because the exact number of surface active sites (hydrogen or oxygen binding sites) is unknown, we estimated the number of surface active sites as the total number of surface sites including Ni, Co, P atoms.

The active sites per real surface area is calculated from the following formula:

$$\text{Number of active sites} = \left(\frac{\text{Number of surface atoms / unit cell}}{\text{Volume / unit cell}}\right)^{\frac{2}{3}}$$

(4)

We calculated the number of active site per real surface area for each phase based on their unit cell volumes (see figures below). XRD measurement confirmed that CoP$_x$ is composed by Co$_2$P and CoP (**Figure S1**). In the same way, NiP$_x$ is composed by Ni$_2$P and NiP. To simplify the computation, we hypothesize the content ratio of (TM)$_2$P and (TM)P is 1:2. Additionally, we estimated the structure of NiCo$_2$P$_x$ is same as CoP$_x$, because there are no obvious difference in XRD patterns between CoP$_x$ and NiCo$_2$P$_x$, thus NiCo$_2$P$_x$ can be considered as Co atoms in CoP$_x$ partially replaced by Ni^{2+} and the structure still reserved. Therefore, the number of active sites can be calculated as:

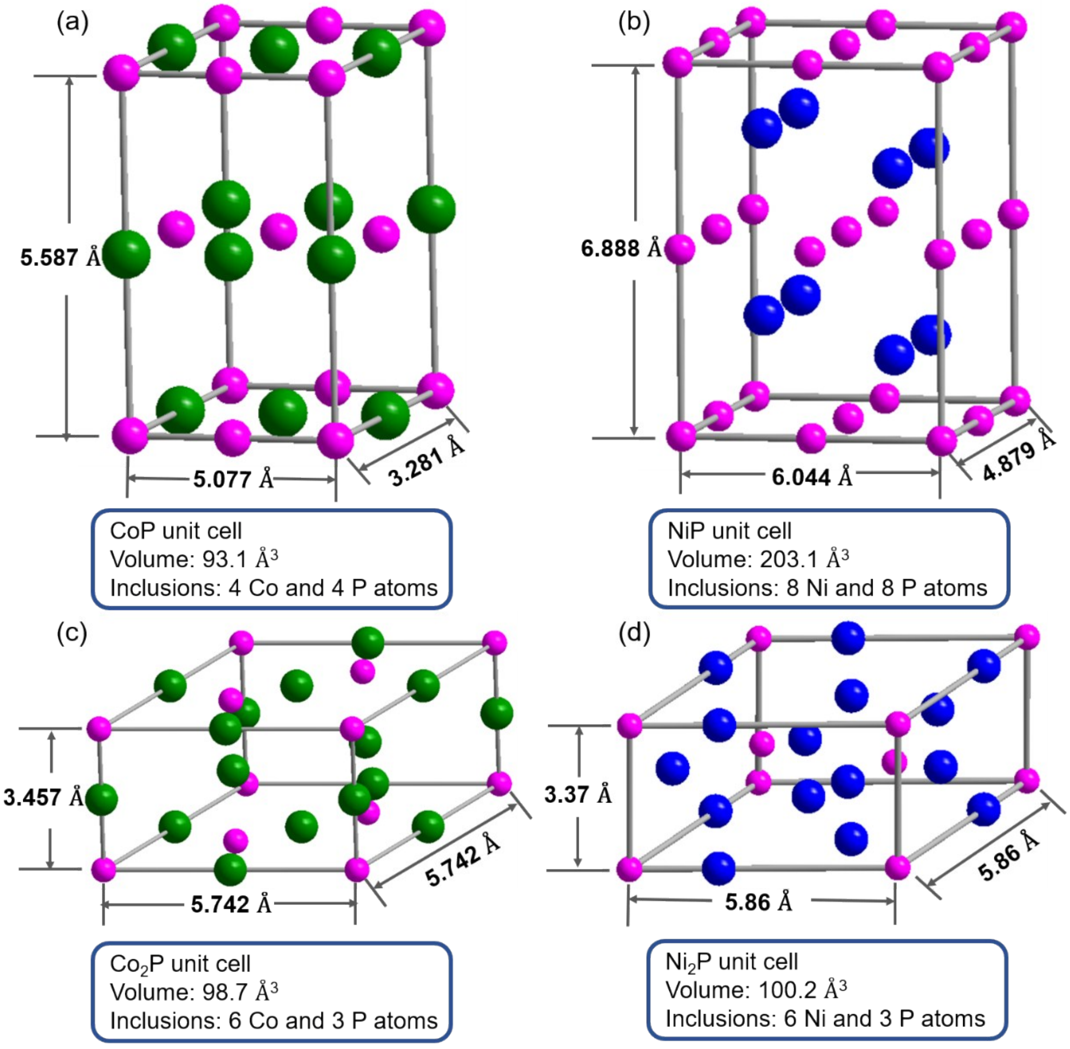

$$\text{Number of active sites(CoP}_x) = \left(\frac{8 \times \frac{1}{2} + 9 \times \frac{1}{3}\ \text{atoms / unit cell}}{93.1 \times \frac{1}{2} + 98.7 \times \frac{1}{3}\ \text{Å}^3\ \text{/ unit cell}}\right)^{\frac{2}{3}} = 1.98 \times 10^{15} \text{atoms}\ cm^{-2} \quad \textbf{(5)}$$

$$\text{Number of active sites(NiP}_x) = \left(\frac{16 \times \frac{1}{4} + 9 \times \frac{1}{3}\ \text{atoms / unit cell}}{203.1 \times \frac{1}{4} + 100.2 \times \frac{1}{3}\ \text{Å}^3\ \text{/ unit cell}}\right)^{\frac{2}{3}} = 1.90 \times 10^{15} \text{atoms}\ cm^{-2} \quad \textbf{(6)}$$

$$\text{Number of active sites(NiCo}_2\text{P}_x) = \left(\frac{8 \times \frac{1}{2} + 9 \times \frac{1}{3}\ \text{atoms / unit cell}}{93.1 \times \frac{1}{2} + 98.7 \times \frac{1}{3}\ \text{Å}^3\ \text{/ unit cell}}\right)^{\frac{2}{3}} = 1.98 \times 10^{15} \text{atoms}\ cm^{-2} \quad \textbf{(7)}$$

Finally, substitute the current density j into formula above, TOF can be calculated as:

$$\text{TOF}_{\text{HER}} = j \times \frac{3.12 \times 10^{15}\ \text{H}_2\ \text{molecules}\ mA^{-1}\ s^{-1}}{\text{Number of active sites} \times A_{ECSA}} \quad \textbf{(8)}$$

$$\text{TOF}_{\text{OER}} = j \times \frac{1.56 \times 10^{15}\ \text{O}_2\ \text{molecules}\ mA^{-1}\ s^{-1}}{\text{Number of active sites} \times A_{ECSA}} \quad \textbf{(9)}$$

1.4.5 *Overall water splitting*

To accomplish the full water electrolysis, $NiCo_2P_x$ /CNTs was dispersed to form a homogeneous suspension as we mentioned above. The ink was then drop-casted onto a square region of nickel foam (1*1 cm) to serve as both anodes and cathodes for overall water splitting device (loading: 1 mg cm_{geo}^{-2}). The nickel foam was treated by diluted HCl solution for 10 hours, then drop the epoxy onto dried nickel foam to form 1*1 cm square region. The electrolyte was 1 M KOH. Before performing the test, catalysts were activated by a chronopotentiometry scan at a constant current density (typically 5-10 mA cm^{-2} for 12 h) to reach a steady state[3]. The stability was examined by the chronoamperometry measurements at a constant current density of 10 mA cm^{-2}. The $NiCo_2P_x$ and Pt/C‖IrO_2 were also tested for comparison. All the data for overall water splitting were presented without *IR*-correction.

1.4.6 *The multi-potential process*

The multi-potential chronopotentiometric process of $NiCo_2P_x$ /CNTs, bulk $NiCo_2P_x$, and Pt/C‖IrO_2 for overall water splitting was performed at initial voltages of 1.54, 1.62, and 1.56 V respectively with an increment of 10 mV per step. The multi-potential chronopotentiometric curves were presented without *IR* correction.

2. Supplementary Figures

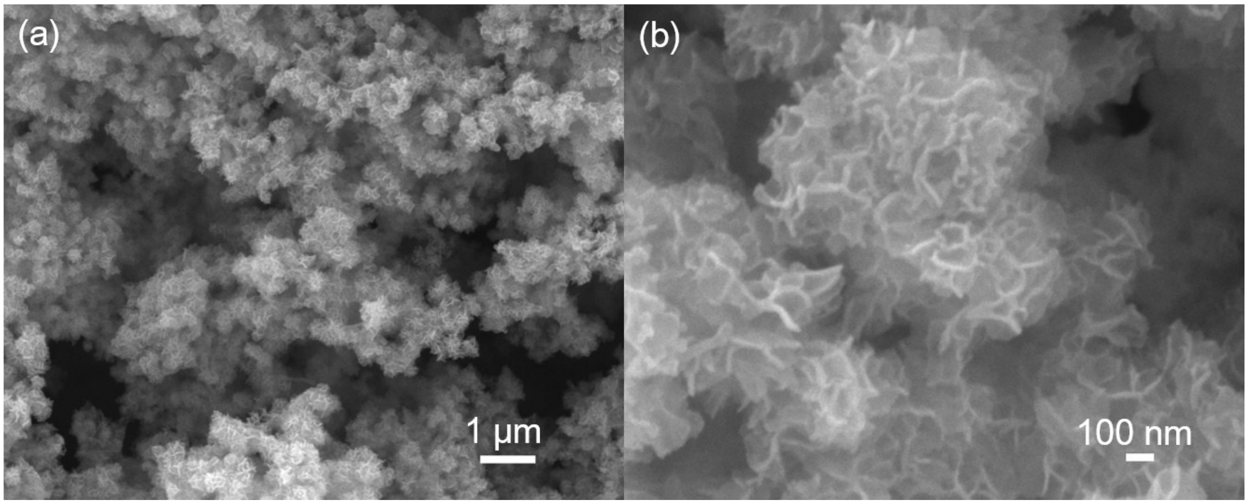

Figure S1. SEM images of the $NiCo_2P_x$/CNTs.

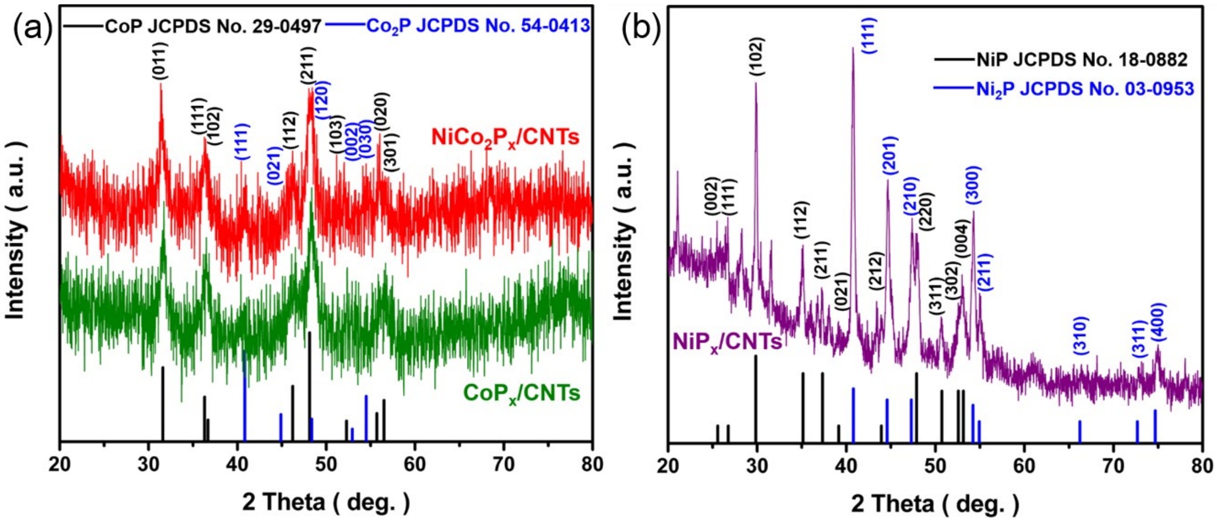

Figure S2. XRD patterns of the (a) $NiCo_2P_x$/CNTs and CoP_x/CNTs, (b)NiP_x/CNTs.

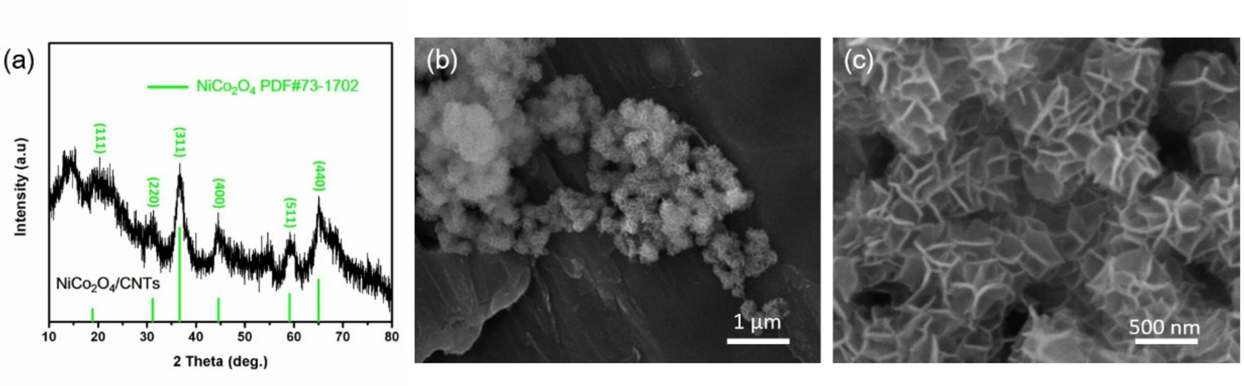

Figure S3. (a) XRD pattern and (b, c) SEM images of the $NiCo_2O_4$/CNTs.

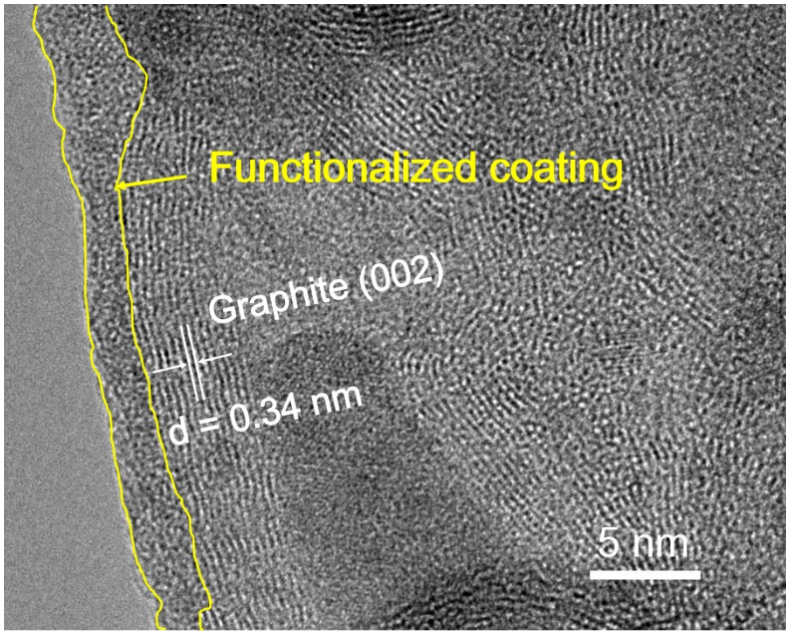

Figure S4. HRTEM image of the $NiCo_2P_x$/CNTs.

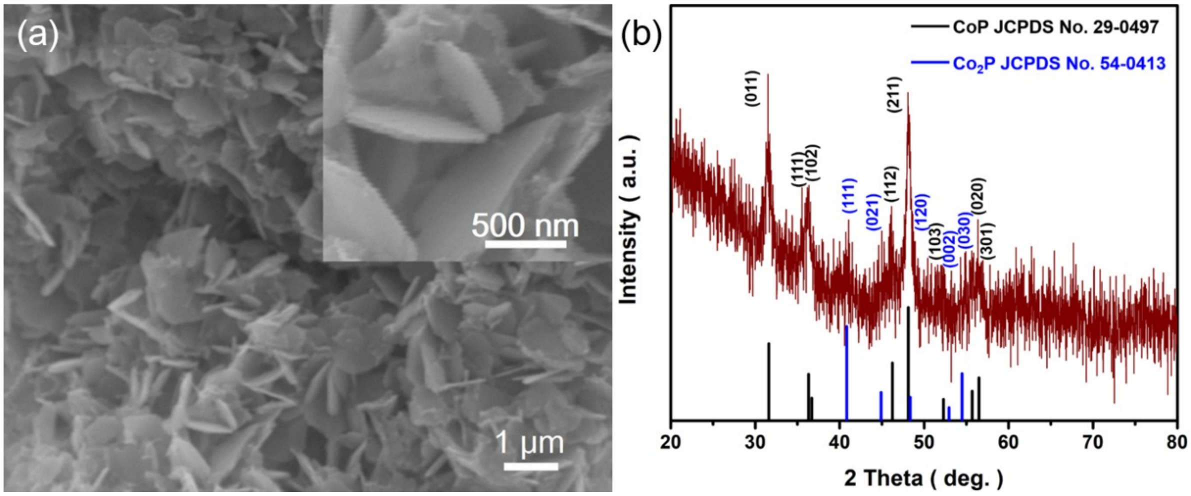

Figure S5. (a) SEM image and (b) XRD pattern of bulk $NiCo_2P_x$.

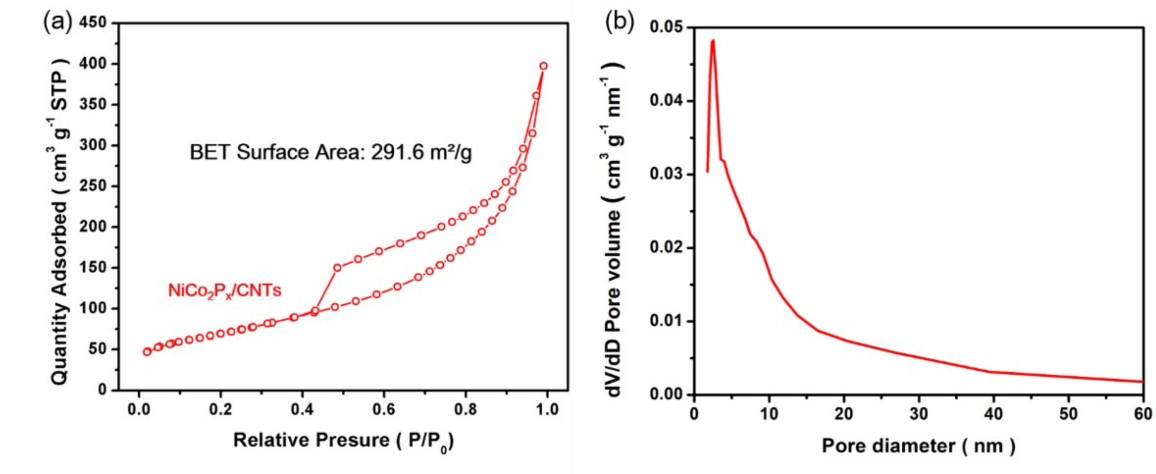

Figure S6. N_2 adsorption-desorption isotherms and (b) the corresponding BJH pore distribution of $NiCo_2P_x$/CNTs.

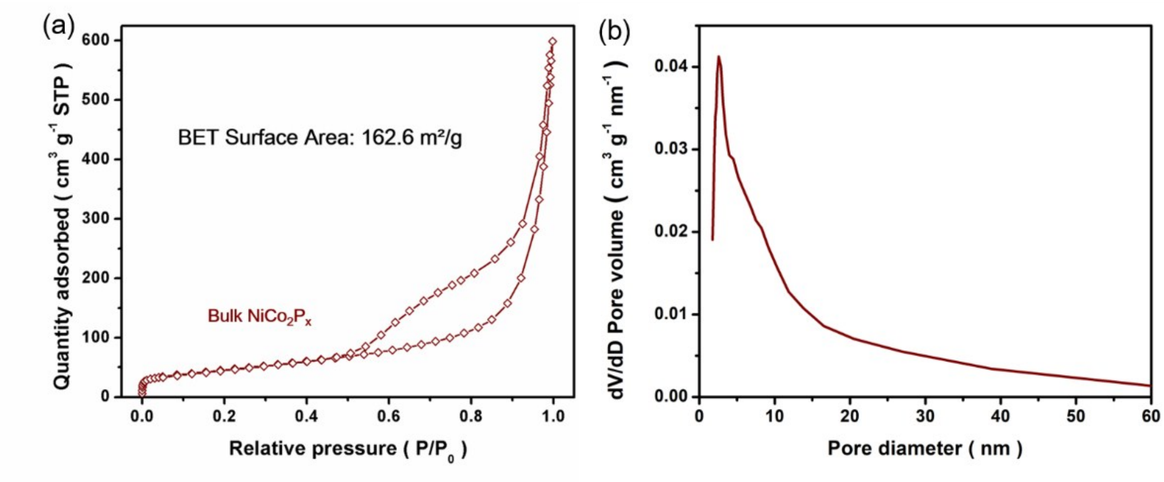

Figure S7. (a) N_2 adsorption-desorption isotherms and (b) the corresponding BJH pore distribution of bulk $NiCo_2P_x$.

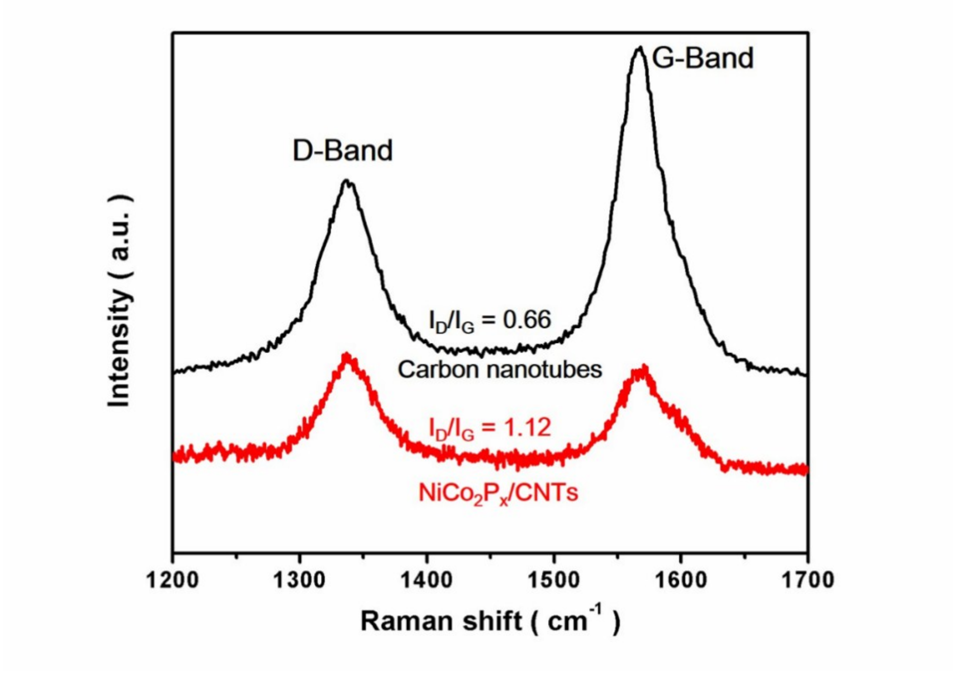

Figure S8. Raman spectra of pristine CNTs and $NiCo_2P_x$/CNTs.

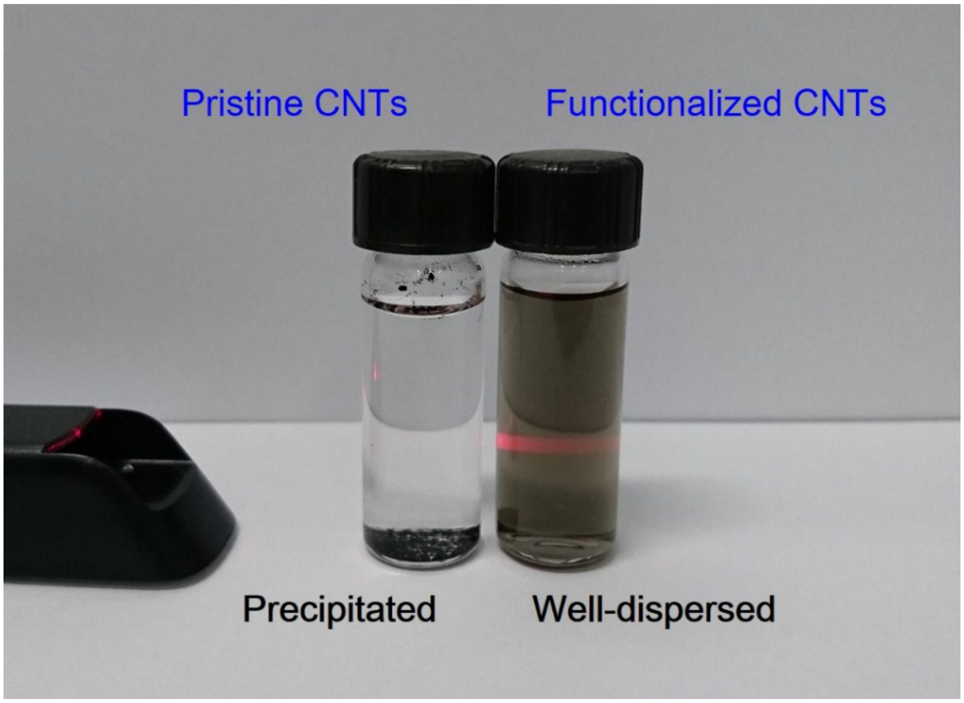

Figure S9. Digital photographs for pristine and functionalized CNTs distributed in aqueous solution showing the Tyndall effect.

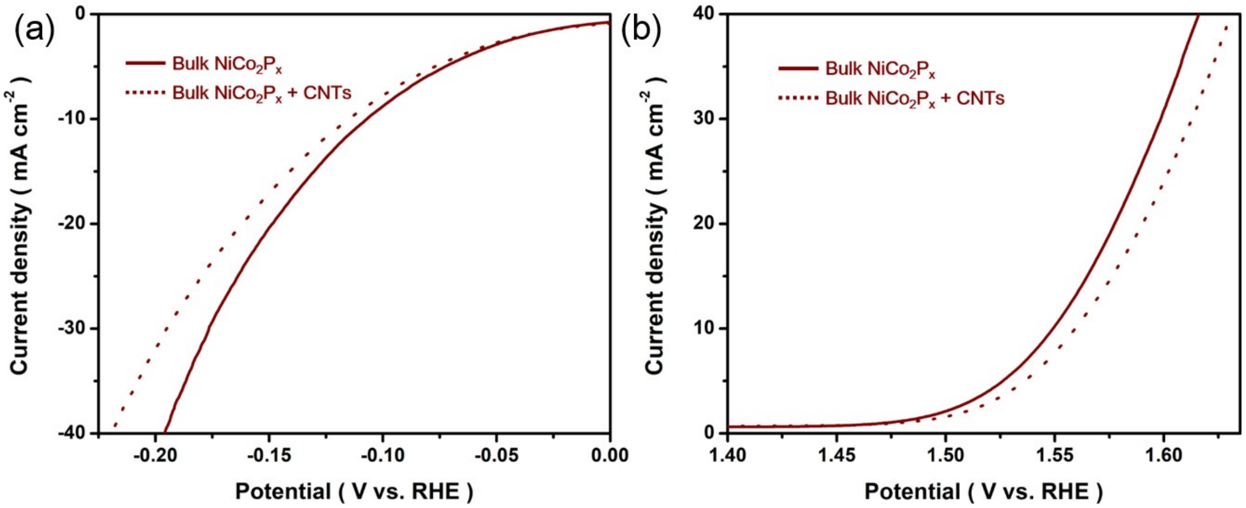

Figure S10. Polarization curves for (a) HER and (b) OER of bulk $NiCo_2P_x$ and bulk $NiCo_2P_x$+CNTs.

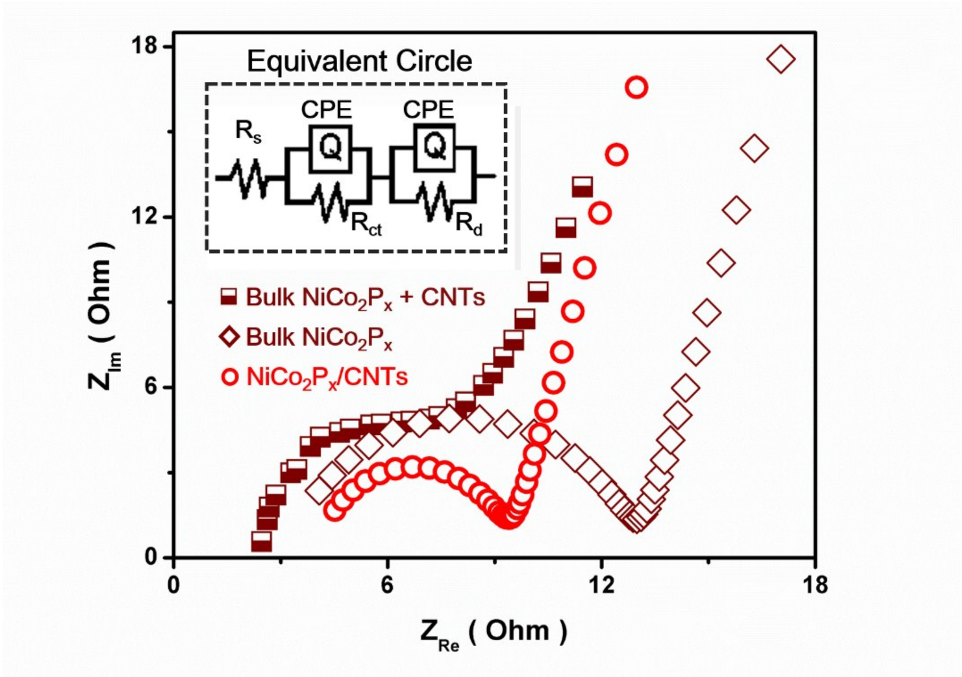

Figure S11. Nyquist plots of bulk $NiCo_2P_x$+CNTs, bulk $NiCo_2P_x$ and $NiCo_2P_x$/CNTs. The inset shows the equivalent circuit diagram.

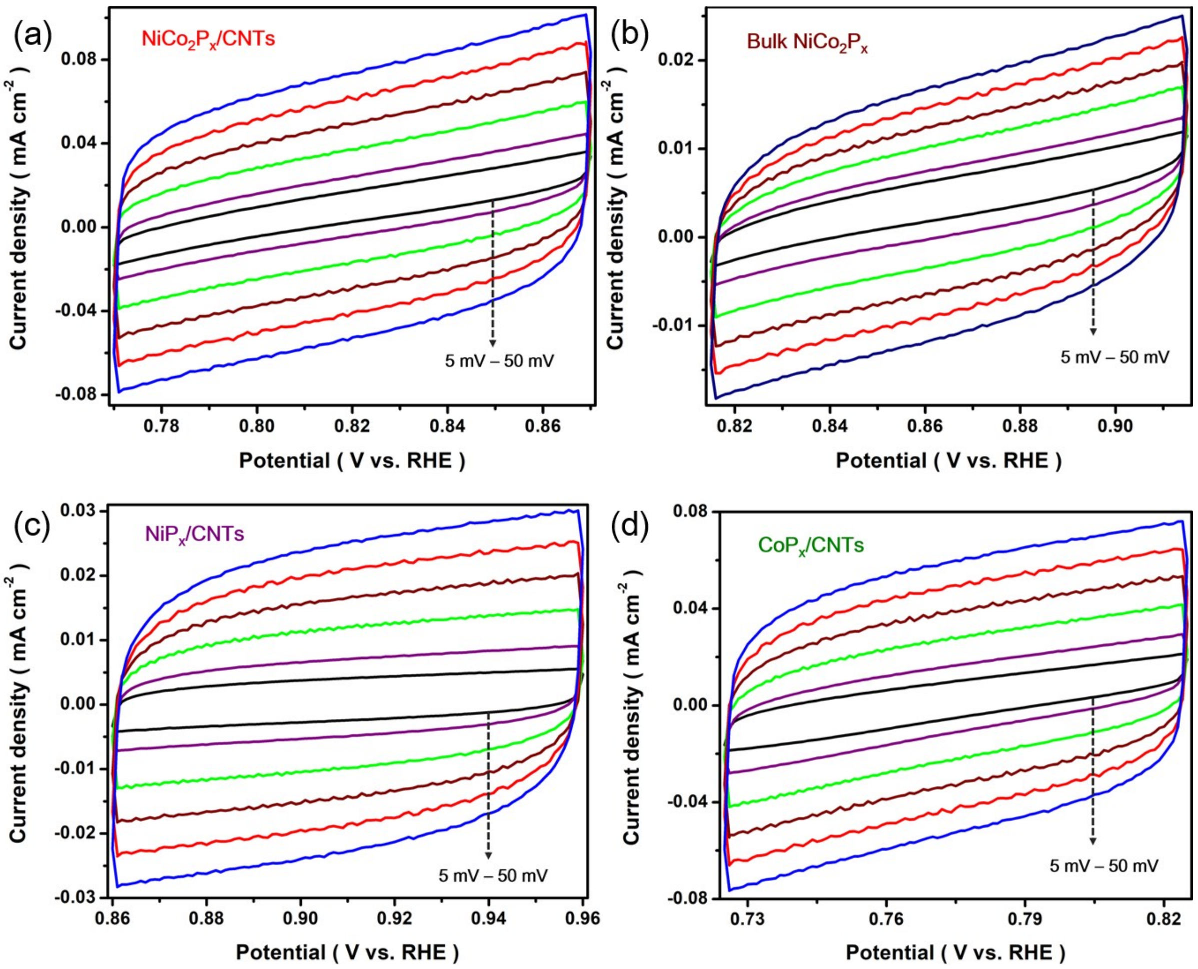

Figure S12. CVs of (a) $NiCo_2P_x$/CNTs, (b) bulk $NiCo_2P_x$, (c) NiP_x/CNTs and (d) CoP_x/CNTs at different scan rates.

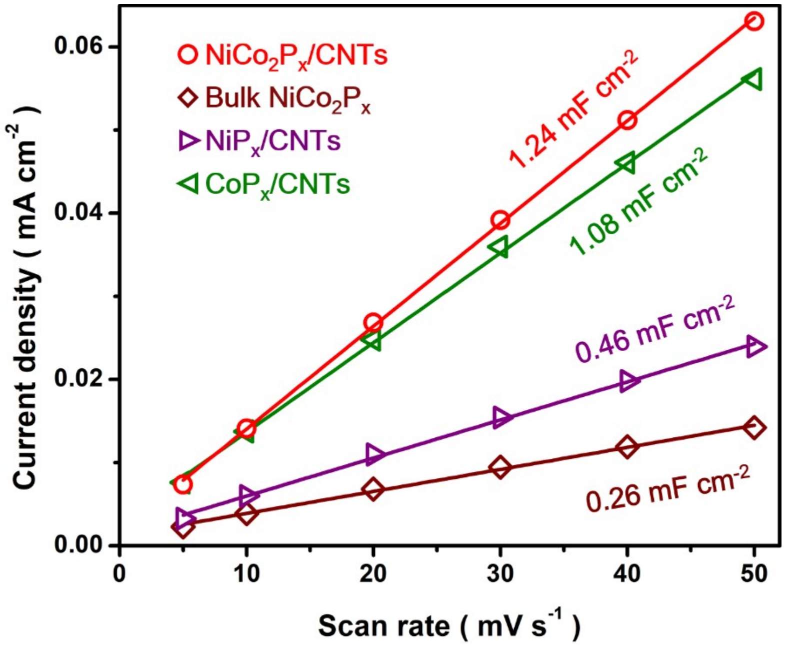

Figure S13. The difference in current density plotted against scan rate of of NiCo$_2$P$_x$/CNTs, bulk NiCo$_2$P$_x$, NiP$_x$/CNTs and CoP$_x$/CNTs for estimating the double layer capacitances.

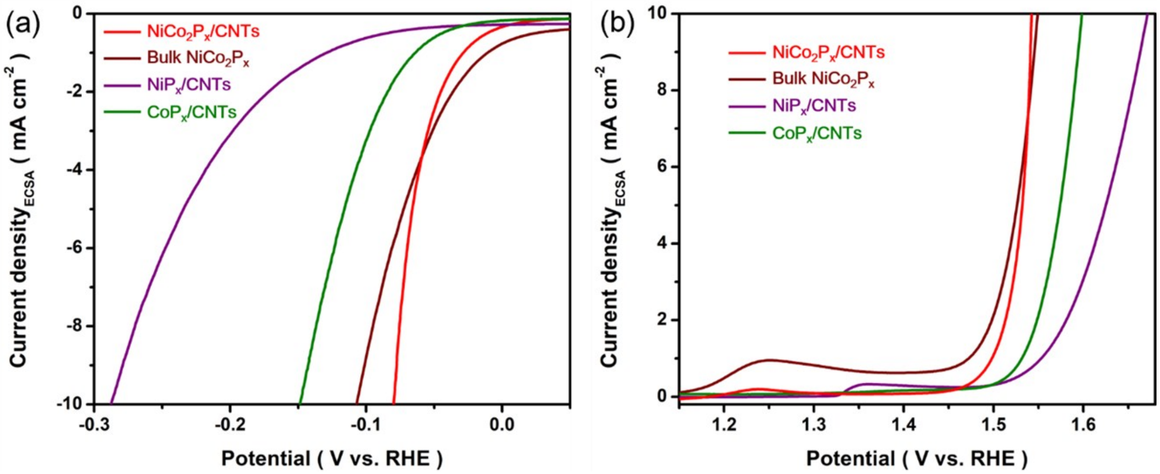

Figure S14. Polarization curves for (a) HER and (b) OER normalized by ECSA of NiCo$_2$P$_x$/CNTs, bulk NiCo$_2$P$_x$, NiP$_x$/CNTs and CoP$_x$/CNTs.

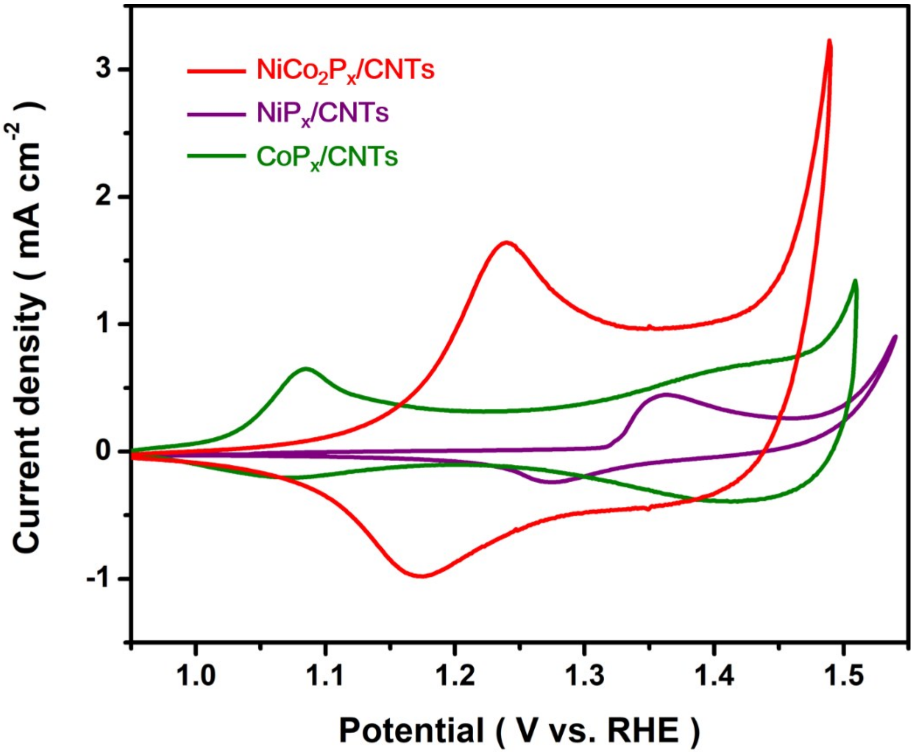

Figure S15. The comparison among CV curves of NiCo$_2$P$_x$/CNTs, NiP$_x$/CNTs and CoP$_x$/CNTs.

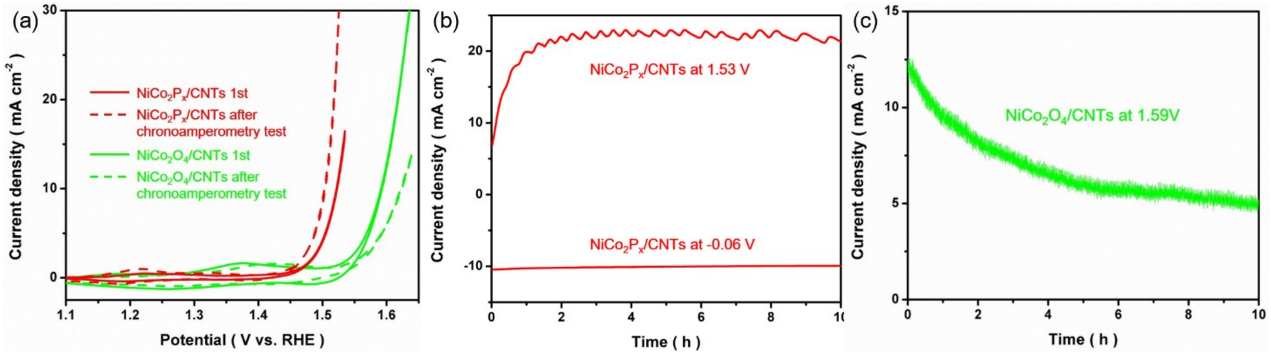

Figure S16. (a) CV curves before and after chronoamperometry test of NiCo$_2$P$_x$/CNTs and NiCo$_2$O$_4$/CNTs. Chronoamperometric curves of (b) NiCo$_2$P$_x$/CNTs and (c) NiCo$_2$O$_4$/CNTs.

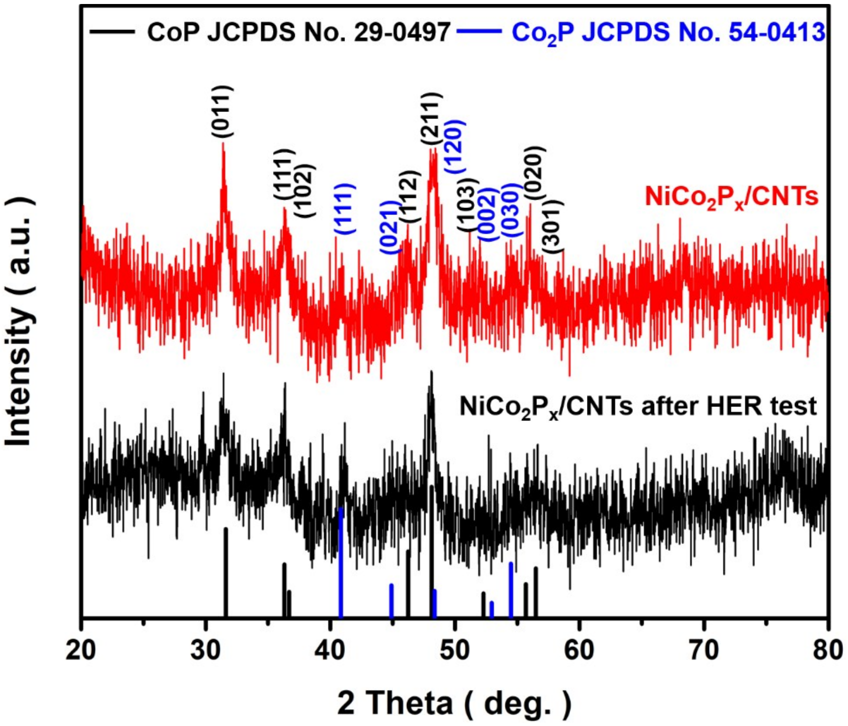

Figure S17. XRD patterns of the $NiCo_2P_x$/CNTs before and after HER tests.

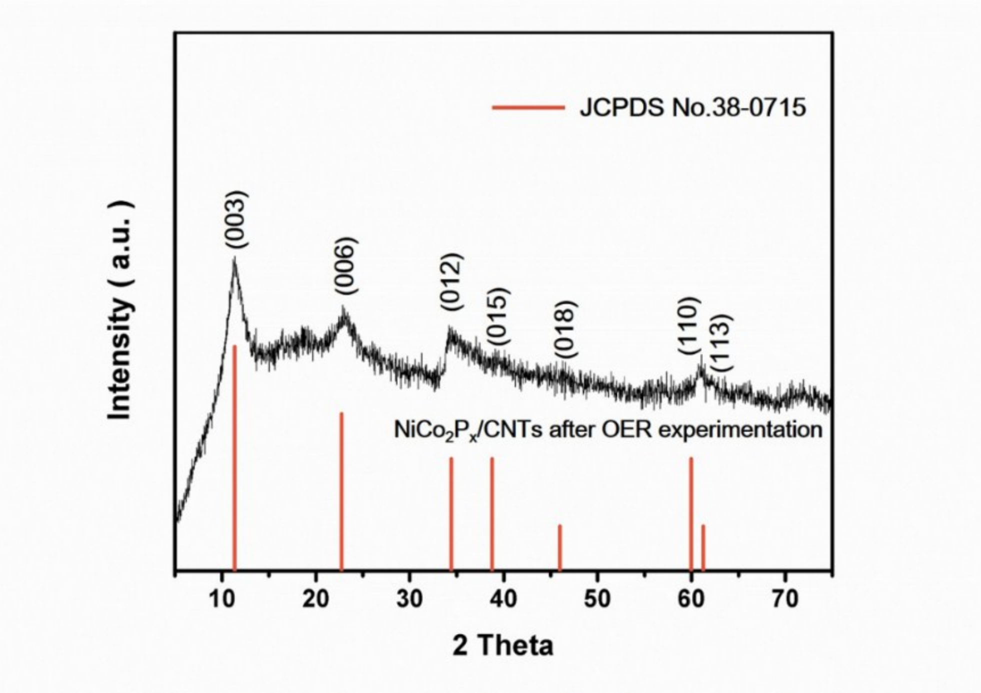

Figure S18. XRD pattern of the $NiCo_2P_x$/CNTs after OER tests.

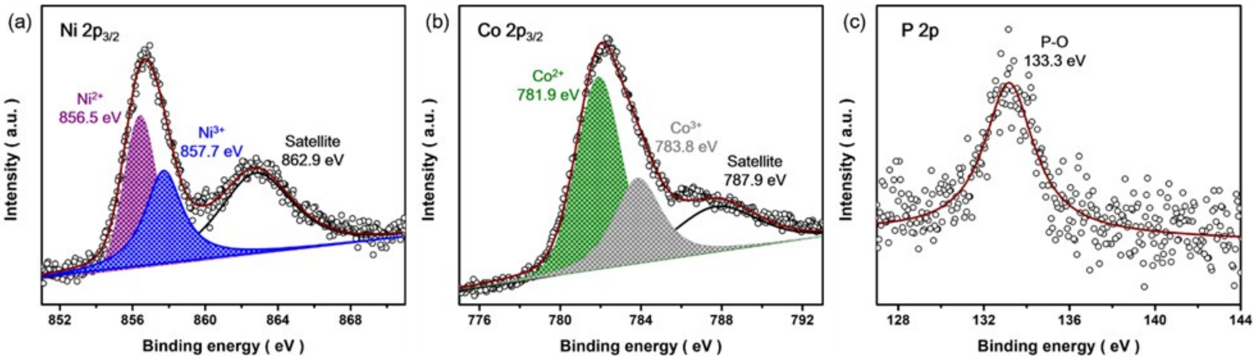

Figure S19. XPS spectra for (a) Ni $2p_{3/2}$, (b) Co $2p_{3/2}$, (c) P 2p of $NiCo_2P_x$/CNTs after stability test.

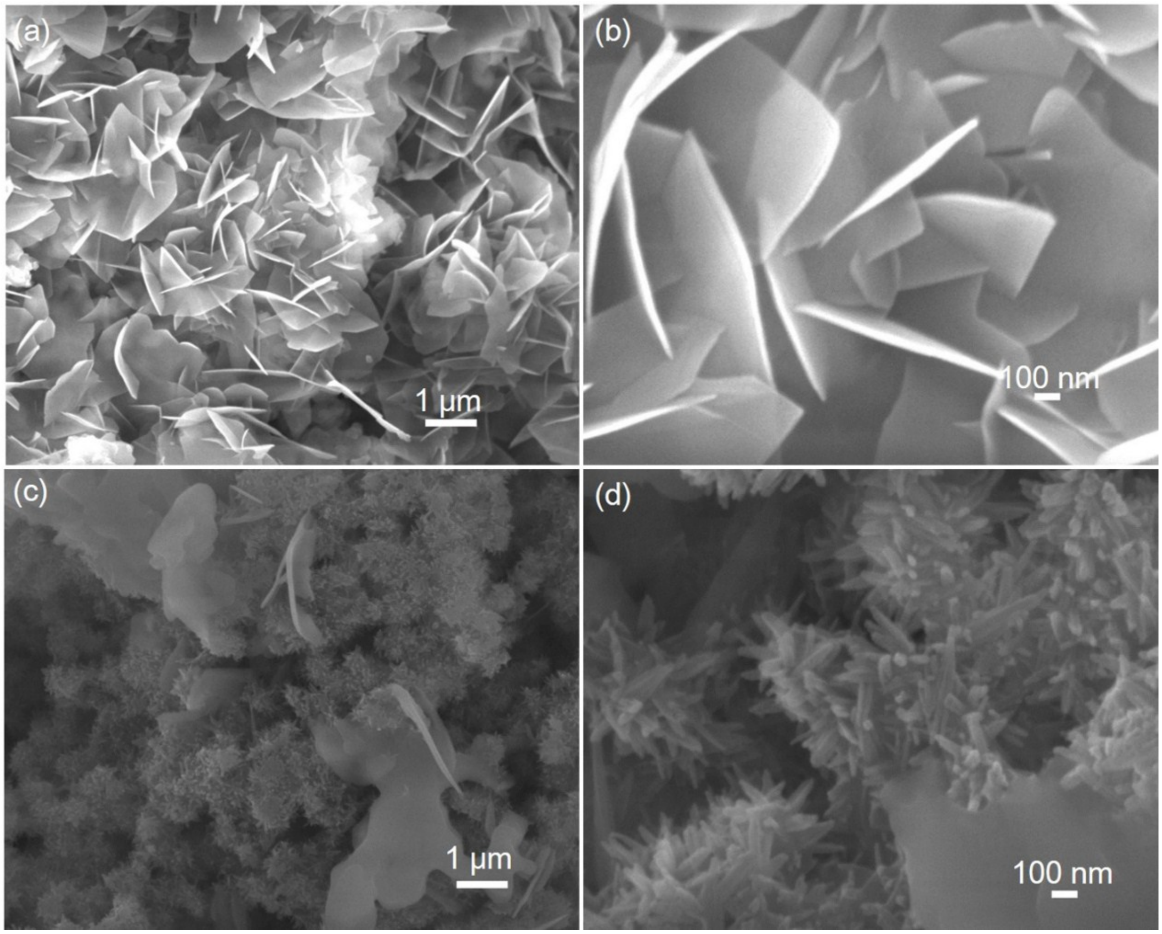

Figure S20. SEM images of (a, b) post-OER and (c, d) post-HER $NiCo_2P_x$/CNTs after 48 h stability tests.

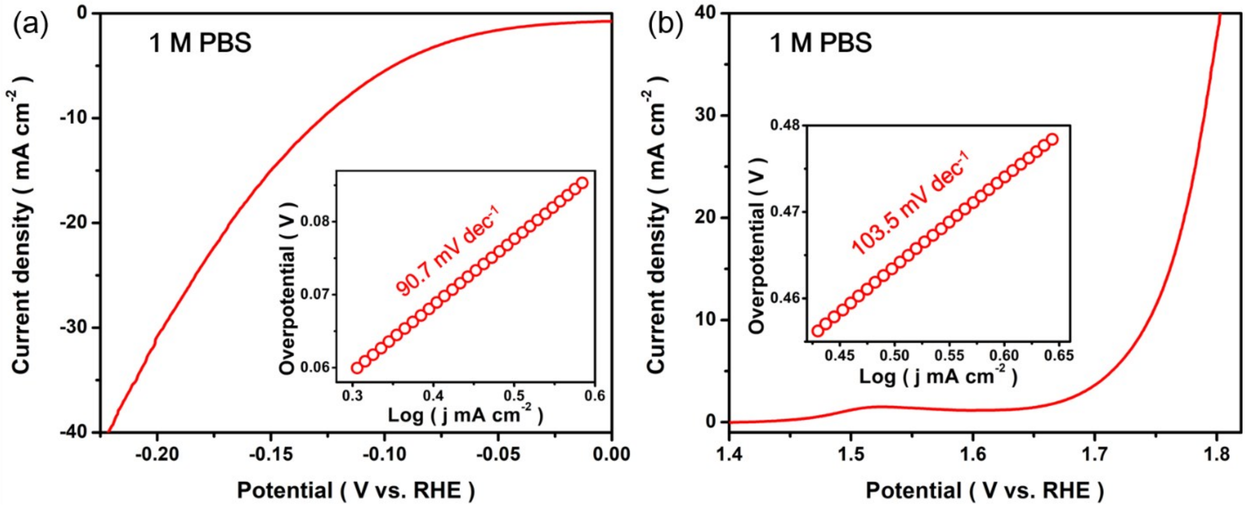

Figure S21. The polarization curves for (a) HER, (b) OER and (inset) corresponding Tafel plots of $NiCo_2P_x$/CNTs in 1 M PBS.

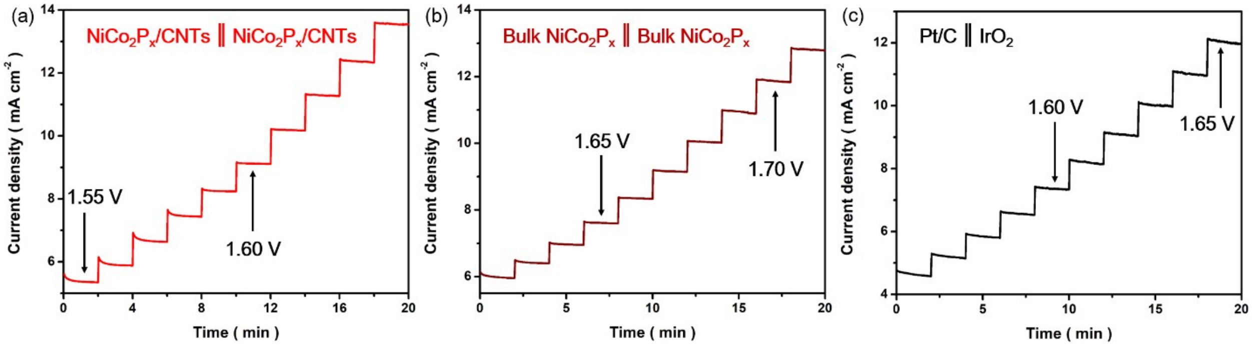

Figure S22. The multi-potential chronoamperometric curves of (a) $NiCo_2P_x$/CNTs, (b) bulk $NiCo_2P_x$, and (c) Pt/C‖IrO_2 for overall water splitting.

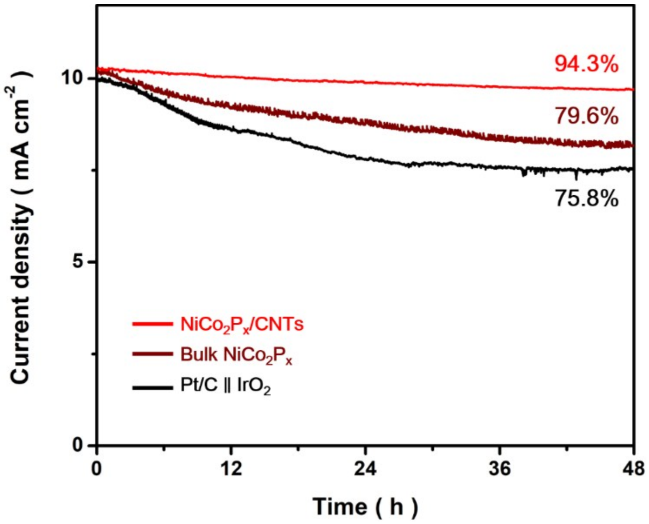

Figure S23. Stability tests of $NiCo_2P_x$/CNTs, bulk $NiCo_2P_x$, and Pt/C‖IrO_2.

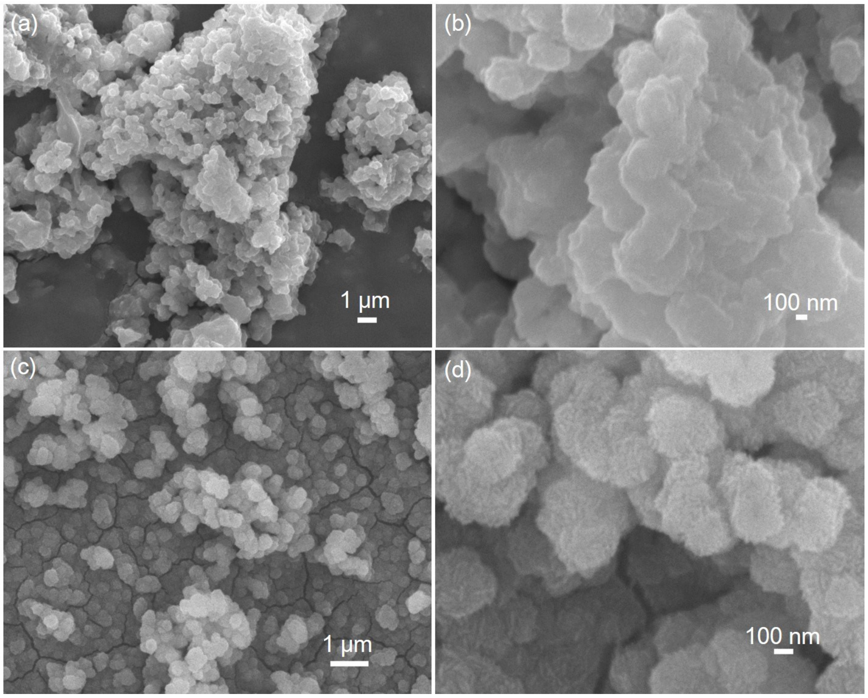

Figure S24. SEM images of bulk $NiCo_2P_x$ after 48 h stability test for (a, b) OER and (c, d) HER.

Table S1 Element content of Ni, Co, P, C and O in $NiCo_2P_x$/CNTs and bulk $NiCo_2P_x$ calculated by XPS scan.

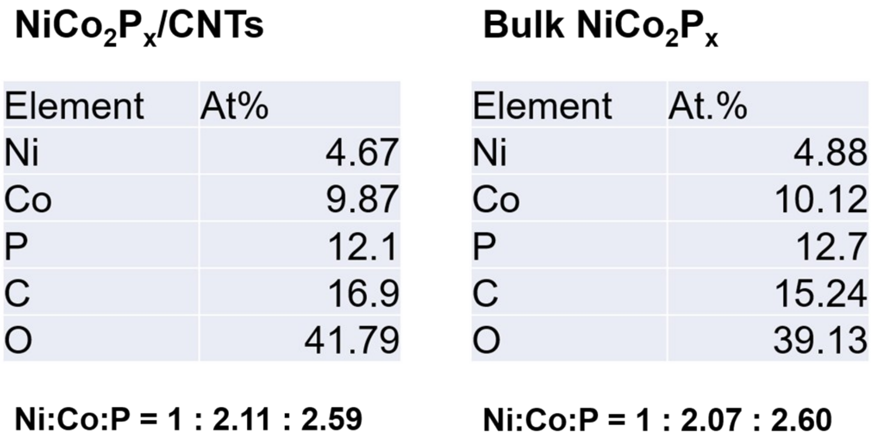

NiCo$_2$P$_x$/CNTs

Element	At%
Ni	4.67
Co	9.87
P	12.1
C	16.9
O	41.79

Ni:Co:P = 1 : 2.11 : 2.59

Bulk NiCo$_2$P$_x$

Element	At.%
Ni	4.88
Co	10.12
P	12.7
C	15.24
O	39.13

Ni:Co:P = 1 : 2.07 : 2.60

Table S2 Comparison of HER performance of catalysts in this work and other reported transition metal electrocatalysts in alkaline media.

Catalyst	η_{10} (mV)	Tafel slope (mV dec^{-1})	Electrolyte	Refference
$NiCo_2P_x$/CNTs	**47**	**56**	**1 M KOH**	**This work**
bulk $NiCo_2P_x$	**107**	**85.5**	**1 M KOH**	**This work**
$NiCo_2O_4$/CNTs	**415**	**81**	**1 M KOH**	**This work**
CoP nanowire arrays	209	129	1 M KOH	J. Am. Chem. Soc., 2014, 136, 7587-7590
NiP_2 nanosheet arrays	102	65	1 M KOH	Nanoscale, 2014, 6, 13440-13445.
Ni_5P_4/Nickel foil	150	53	1 M KOH	Angew. Chem. Int. Ed., 2015, 54, 12361-12365.
Ni-Co-P nanocubes	150	60.6	1 M KOH	Chem. Commun., 2016, 52, 1633-1636
Ni_5P_4-MP	49	98	1 M KOH	Energy Environ. Sci. 2015, 8, 1027
Ni_2P	69	118	1 M KOH	Energy Environ. Sci. 2015, 8, 1027
CoP/Carbon	95	60	1 M KOH	ChemSusChem 2016, 9, 472
CoP/rGO	150	38	1 M KOH	Chem. Sci. 2016, 7, 1690
NiFe LDH/NF	210	/	1 M KOH	Science, 2014, 345, 1593
Co_xPO_4/CoP	380	/	1 M KOH	Adv Mater 2015, 27, 3175.
Co/CoP	94	42	1 M KOH	Angew Chem Int Edit 2015, 54, 6251.
NiO/Ni-CNT	80	51	1 M KOH	Nat. Commun. 2014, 5, 4695
CoSe/Ti	121	84	1 M KOH	Chem. Commun. 2015, 51, 16683
Ni_2P/Ni foam	~65	50	1 M KOH	ACS Appl. Mater. Interfaces 2015, 7, 2376.

Table S3 Comparison of OER performance of catalysts in this work and other reported transition metal electrocatalysts in alkaline media.

Catalyst	η_{10} (mV)	Tafel slope (mV dec^{-1})	Electrolyte	Refference
$NiCo_2P_x$/CNTs	**284**	**50.3**	**1 M KOH**	**This work**
bulk $NiCo_2P_x$	**320**	**69.9**	**1 M KOH**	**This work**
$NiCo_2O_4$/CNTs	**503**	**66.5**	**1 M KOH**	**This work**
$Co_{0.85}Se$/CC	324	85	1 M KOH	Adv. Mater. 2015, 28, 77
Co_3O_4@C/CP	370	70	1 M KOH	Nano Energy 2016, 25, 42
CoCo LDH	393	59	1 M KOH	Nat. Commun. 2014, 5, 4477
CoP/C	320	71	1 M KOH	ACS Catal. 2015, 5, 6874
CoP/rGO	340	66	1 M KOH	Chem. Sci. 2016, 7, 1690
N-doped graphene-CoO	340	67	1 M KOH	Energy Environ. Sci. 2014, 7, 609.
NiFe LDH/NF	240	/	1 M KOH	Science, 2014, 345, 1593
Co/P films	345	47	1 M KOH	Angew. Chem. Int. Ed. 2015, 54, 6251-6254
NiCo-LDH	~420 mV	113	0.1 M KOH	Journal of Power Sources 2015, 278, 445-451
Co_3O_4/Co_3O_4 DSNCs	340	88	0.1 M KOH	J. Am. Chem. Soc.2015, 137, 5590−5595

Reference cited in Supporting Information:

1. W. S. Hummers and R. E. Offeman, *J. Am. Chem. Soc.*, 1958, **80**, 1339-1339.
2. H. Liang, A. N. Gandi, D. H. Anjum, X. Wang, U. Schwingenschlogl and H. N. Alshareef, *Nano Lett.*, 2016, **16**, 7718-7725.
3. X. Xu, F. Song and X. Hu, *Nat. Commun.*, 2016, **7**, 12324.